The Cryosphere Discuss., https://doi.org/10.5194/tc-2018-130
Manuscript under review for journal The Cryosphere
Discussion started: 11 July 2018

The Cryosphere Discussions
Open Access
EGU

Brief communication: An Ice surface melt scheme including the diurnal cycle of solar radiation

Uta Krebs-Kanzow[1], Paul Gierz[1], and Gerrit Lohmann[1]

[1]Alfred Wegener Institute Helmholtz Centre for Polar and Marine Research, Bremerhaven, Germany

Correspondence: Uta Krebs-Kanzow (uta.krebs-kanzow@awi.de)

Abstract.

We propose a surface melt scheme for glaciated land surfaces, which only requires monthly mean short wave radiation and temperature as inputs, yet implicitly accounts for the diurnal cycle of short wave radiation. The scheme is deduced from the energy balance of a daily melt period which is defined by a minimum solar elevation angle. The scheme yields a better spatial representation of melting than common empirical schemes when applied to the Greenland Ice Sheet, using a 1948-2016 regional climate and snow pack simulation as a reference. The scheme is physically constrained and can be adapted to other regions or time periods.

1 Introduction

The surface melt of ice sheets, ice caps and glaciers results in a freshwater runoff that represents an important freshwater source and directly influences the sea level on centennial to glacial-interglacial time scales. Surface melt rates can be determined from direct local measurements (e.g. Ahlstrom et al., 2008; Falk et al., 2018). On a larger scale, melt rates can be separated from integral observations such as the the World Glacier Monitoring Service (WGMS) (Zemp et al., 2015, and references therein) or the mass changes of ice sheets detected by the Gravity Recovery and Climate Experiment (GRACE) (Tapley et al., 2004; Wouters et al., 2014), which requires additional information on other components of the mass balance, such as basal melting, accumulation, sublimation and refreeze (Sasgen et al., 2012; Tedesco and Fettweis, 2012). In principal, the surface melt rate can be deduced from the net heat flux into the surface layer, as soon as the ice surface has been warmed to the melting point. For low solar elevation angles, however, the net heat flux into the surface layer usually becomes negative, the ice surface cools below the melting point and melting ceases. Consequently, energy balance modelling provides reliable surface melt rates only if sub-daily changes in ice surface temperature and nocturnal freezing are taken into account. Where sub-daily energy balance modelling is not feasible, surface melt is often estimated from empirical schemes. A common approach is the positive degree-day method as formulated e.g. in Reeh (1989). This particularly simple aproach linearly relates mean melt rates to positive degree-days, PDD, in which PDD refers to the temporal integral of near surface temperatures T exceeding the melting point. The PDD-scheme is computational inexpensive and requires only seasonal or monthly near surface air temperatures. Consequently, it has been applied in the context of long climate simulations (e.g. Charbit et al., 2013; Ziemen et al., 2014; Heinemann et al., 2014; Roche et al., 2014; Gierz et al., 2015) or paleo-temperature reconstructions (e.g. Box, 2013;

The Cryosphere Discuss., https://doi.org/10.5194/tc-2018-130
Manuscript under review for journal The Cryosphere
Discussion started: 11 July 2018

Wilton et al., 2017). Another empirical aproach, the enhanced temperature-index method, ETIM (Pollard, 1980), additionally includes solar radiation. This aproach is often chosen when the influence of solar radiation is changing over orbital time scales (e.g. van den Berg et al., 2008; de Boer et al., 2013) or is enhanced over debris-covered glaciers (e.g. Pellicciotti et al., 2005; Carenzo et al., 2016). Both, the ETIM and the PDD-scheme, incorporate parameters, which require a local calibration and which are not necessarily valid under different climate conditions. Additionally, Bauer and Ganopolski (2017) demonstrate that the PDD-scheme fails to drive glacial-interglacial ice volume changes as it cannot account for albedo feedbacks. An alternative aproach could be to modify and simplify energy balance models in a way that reduces their data requirements and computational costs. Krapp et al. (2017) have formulated an energy balance model which can be used with daily forcing and which still is relatively complex. This model implicitly accounts for the sub-daily temperature variations in the surface layer of the ice by making general assumptions about their shape and amplitude. In the following, we deduce a more simplified scheme from the energy balance, which is formally similar to the ETIM but incorporates physically constrained parameters. This new scheme implicitly resolves the diurnal cycle of radiation and only requires monthly means of temperature and solar radiation as input. In a first application on the Greenland Ice Sheet, GrIS, we use a simulation of Greenland's climate of the years 1948 to 2016 with the state-of-the-art regional climate and snow pack model MAR (version 3.5.2 forced with reanalysis data from the National Centers for Environmental Prediction–National Center for Atmospheric Research (NCEP) for the years 1948-2016, Kalnay et al., 1996; Fettweis et al., 2017) as a reference.

2 The daily melt period and its energy balance

The temperature of a surface layer of ice T_i must rise to the melting point T_0 before the net energy uptake Q of a surface layer can result in a surface melt rate M. In the following, we define background melt conditions on a monthly scale and melt periods on a daily scale.

The near surface air temperature T_a usually does not exceed T_0 if (after winter) the ice is still too cold to aproach T_0 during daytime, so that, on a monthly scale surface air temperatures $\overline{T}_a$ (with the bar denoting monthly means hereafter) can serve as an indicator for background melting conditions. In the following we assume that monthly mean melt rates $\overline{M} > 0$ only occur if $\overline{T}_a > T_{min}$, where T_{min} is a typical threshold temperature to allow melt.

The daily melt period shall be that part of a day, during which $T_i = T_0$ and $Q \geq 0$. Here, this period is assumed to be centered around solar noon, so that it is also defined by the period Δt_Φ, during which the sun is above a certain elevation angle Φ. Further, we define the ratio between the mean solar radiation during the melt period, SW_Φ, and the mean daily solar radiation, SW_0, as

$$q_\Phi = \frac{SW_\Phi}{SW_0} \tag{1}$$

Both Δt_Φ and q_Φ depend on the diurnal cycle of short wave radiation and can be expressed as functions of latitude and time for any elevation angle Φ, including parameters of the Earth's orbit around the sun. Δt_Φ and q_Φ will be derived in Sect. 2.1.

During the melt period, Q_Φ provides energy for fusion and results in a melt rate, which, averaged over a full day Δt, amounts

The Cryosphere Discuss., https://doi.org/10.5194/tc-2018-130
Manuscript under review for journal The Cryosphere
Discussion started: 11 July 2018

to

$$M = \frac{Q_\Phi \Delta t_\Phi}{\Delta t \rho L_f} \tag{2}$$

with latent heat of fusion $L_f = 3.34 \times 10^5\,\mathrm{J\,kg^{-1}}$ and the density of liquid water $\rho = 1000\,\mathrm{kg\,m^{-3}}$. The energy uptake of the surface layer is

$$Q_\Phi = (1-A)SW_\Phi + \epsilon_i LW\downarrow - LW\uparrow + R \tag{3}$$

with surface albedo A, long wave emissivity of ice $\epsilon_i = 0.95$, downward and upward longwave radiation $LW\downarrow$ and $LW\uparrow$ respectively and the sum of all non radiative heat fluxes R. Per definitionem,

$$LW\uparrow = \epsilon_i \sigma T_0^4 \tag{4}$$

is valid during the melting period, with $\sigma = 5.67 \times 10^{-8}\,\mathrm{W\,m^{-2}\,K^{-4}}$ being the Stefan–Boltzmann constant. Further $T_a - T_0$ will be small relative to T_0 so that $LW\downarrow$ can be linearized to

$$LW\downarrow = \epsilon_a \sigma T_a^4 \approx \epsilon_a \sigma (T_0^4 + 4T_0^3(T_a - T_0)) \tag{5}$$

with ϵ_a being the emissivity of air. Neglecting latent heat fluxes and heat fluxes to the subsurface and assuming R to be dominated by the sensible heat flux, we parameterize $R = \beta(T_a - T_0)$, with the turbulent heat transfer coeficient β. The turbulent heat transfer coeficient depends on wind speed and near surface temperature stratification and is estimated to be in the range of 7 to $20\,\mathrm{W\,m^{-2}\,K^{-1}}$ on melting surfaces (Braithwaite, 1995, and references therein). Rewriting Eq. (3) for monthly means, we replace $(T_a - T_0)$ with PDD($\overline{T}_a$). $PDD(\overline{T}_a)$ serves here as an estimate for the temperatures effectively causing melt (Krebs-Kanzow et al., 2018) and is approximated from monthly mean near surface temperature $\overline{T}_a$ and a constant standard deviation of $5\,^\circ\mathrm{C}$ as in Braithwaite (1985). The above approximations and assumptions then yield an implicitly diurnal Energy Balance Model (dEBM), which only requires monthly mean temperatures and solar radiation as atmospheric forcing, while albedo may be parameterized as in common surface mass balance schemes (e.g. Krapp et al., 2017):

$$\overline{M} \approx \left(q_\Phi (1-A)\overline{SW}_0 + c_1 PDD(\overline{T}_a) + c_2\right) \frac{\Delta t_\Phi}{\Delta t \rho L_f} \tag{6}$$

where

$$\begin{aligned} c_1 &= \epsilon_i \sigma 4T_0^3 + \beta \\ c_2 &= -\epsilon_i \sigma T_0^4 + \epsilon_a \epsilon_i \sigma (T_0^4) \end{aligned} \tag{7}$$

for any month that complies with the background melting condition $\overline{T}_a > T_{min}$.

Finally, we use that $M = 0$ in the moment when the sun passes Φ and formulate the instantanous energy balance anlogously to Eq. (6) as

$$(1-A)\sin\Phi S_0 + c_1(T_a(\Phi) - T_0) + c_2 = 0. \tag{8}$$

The Cryosphere Discuss., https://doi.org/10.5194/tc-2018-130
Manuscript under review for journal The Cryosphere
Discussion started: 11 July 2018

with S_0 being the irradiance normal to a surface at the bottom of the atmosphere and the instantanous air temperature $T_a(\Phi)$. Assuming that $T_a(\Phi) \approx T_0$ and using a typical S_0 we can estimate

$$\Phi = \arcsin \frac{-c_2}{(1-A)S_0} \tag{9}$$

independent of time or location.

2.1 Derivation of Δt_Φ and q_Φ

The derivation of Δt_Φ and q_Φ is based on spherical trigonometry and fundamental astronomic considerations which, for instance, are discussed in detail in Liou (2002). The elevation angle ϑ of the sun changes throughout a day according to

$$\sin\vartheta = \sin\phi\sin\delta + \cos\phi\cos\delta\cos h(\vartheta) \tag{10}$$

with the latitude ϕ, the solar inclination angle δ and the hour angle h.

The time which the sun spends above an elevation angle ϑ then is

$$\Delta t_\vartheta = \frac{\Delta t}{\pi} h(\vartheta) = \frac{\Delta t}{\pi} \arccos \frac{sin\vartheta - \sin\phi\sin\delta}{\cos\phi\cos\delta}. \tag{11}$$

At the top of the atmosphere (TOA) the mean solar radiation during the period which the sun spends above a certain elevation angle ϑ is

$$\widehat{SW}_\vartheta = \frac{\widehat{S}}{\Delta t_\vartheta} \left(h(\vartheta)\sin\phi\sin\delta + (\cos\phi\cos\delta\sin h(\vartheta))\right) \tag{12}$$

with $\widehat{S}$ being the TOA solar radiation on a surface perpendicular to its rays. $\widehat{S}$ is seasonally varying due to the eccentricity of the Earth's orbit. If we assume surface solar radiation to be proportional to the top-of-atmosphere radiation throughout a day (i.e. there is no diurnal cycle in the transmissivity of the atmosphere) we can calculate the ratio between the mean short wave radiation during the melt period SWD_Φ and the mean daily downward short wave radiation SWD_0 also at the surface:

$$q_\Phi = \frac{h(\Phi)\sin\phi\sin\delta + \cos\phi\cos\delta\sin h(\Phi)}{h(0)\sin\phi\sin\delta + \cos\phi\cos\delta\sin h(0)} \frac{\Delta t}{\Delta t_\Phi}. \tag{13}$$

3 First evaluation of the scheme

Choosing $\beta = 10\,\mathrm{W\,m^{-2}\,K^{-1}}$ and using $\epsilon_a = 0.76$ for the present greenhouse gas concentration yields $c_1 = 14.4\,\mathrm{W\,m^{-2}\,K^{-1}}$ and $c_2 = -71.9\,\mathrm{W\,m^{-2}}$. As a background melting condition we here use $\overline{T}_a > -6.5\,\mathrm{K}$. Further, assuming a typical albedo of 0.7 and $S_0 = 600\,\mathrm{W\,m^{-2}}$ in Eq. (9) yields $\Phi = 23.5°$. The new scheme is applied to $\overline{SW}_0$, $PDD(\overline{T}_a)$ and albedo A from a simulation of Greenland's climate (years 1948 to 2016) with the state-of-the-art regional climate and snow pack model MAR (Fettweis et al., 2017). The estimated melt rates are then compared to the respective MAR melt rates.

The Cryosphere Discuss., https://doi.org/10.5194/tc-2018-130
Manuscript under review for journal The Cryosphere
Discussion started: 11 July 2018

Two empirical schemes are tested and evaluated in the same way: a PDD-scheme based on $PDD(\overline{T}_a)$, as defined and calibrated in Krebs-Kanzow et al. (2018) and a common ETIM (Pollard, 1980), which estimates melt as

$$M = ((1-A)\overline{SW}_0 + k_1 PDD(\overline{T}_a) + k_2)\frac{1}{\rho L_f} \tag{14}$$

where $k_1 = 10\,\mathrm{W\,m^{-2}\,K^{-1}}$ and $k_2 = -60.5\,\mathrm{W\,m^{-2}}$ chosen similar to Robinson et al. (2010). We here also use $\overline{T}_a > -6.5\,\mathrm{K}$ as a background melting condition. For better comparison, all schemes have been optimized to reproduce the total annual Greenland surface melt averaged over the entire MAR-simulation of $489\,\mathrm{Gt}$ with a relative bias not exceeding $1\,\%$ (the mean bias is $-4.3\,\mathrm{Gt}$ for the PDD scheme, $0.8\,\mathrm{Gt}$ for the ETIM and $-1.2\,\mathrm{Gt}$ for the dEBM). For the PDD-scheme we use the calibrated parameters from Krebs-Kanzow et al. (2018), in the ETIM we optimized the background melting condition and k_2 and in the dEBM we optimized the background melting condition and the turbulent heat transfer coeficient β within the range given in Braithwaite (1995).

Eqations (6) and (14) appear formally similar, with the first and third term representing the radiative contribution and the second term representing the PDD contribution. However, the respective parameters cannot be compared directly, as the Δt_Φ and q_Φ depend on latitude and month. Δt_Φ and q_Φ modulate the the radiative contribution and Δt_Φ modulates the PDD contribution in Eq. (6). Fig. 1a illustrates the radiative and Fig. 1b the PDD contributions as diagnosed from the MAR simulation in comparison to the respective contribution from the ETIM. On the GrIS the radiative contribution can exceed $40\,\mathrm{mm\,d^{-1}}$ in the summer months and the two schemes appear qualitatively similar. However, a flat ecliptic (going along with long melt periods at high latitudes or with short melt periods in autumn and spring) reduces q_Φ and consequently reduces the radiative contribution in the dEBM. As a result considerable difference between dEBM and ETIM are visible both for short and long melt periods. The PDD contribution of the dEBM appears reduced in comparison to the ETIM and does not exceed $12\,\mathrm{mm\,d^{-1}}$ (Fig. 1b). In the dEBM the PDD contribution becomes more efficient with longer melt periods and would agree with the ETIM for a melt period of 16 hours.

Atmospheric forcing and albedo are here derived from MAR output, and are fully consistent with the MAR melt rates. Consequently, we can evaluate the skill of the considered schemes independent of the quality of the atmospheric forcing and the representation of albedo. On the other hand, we can not evaluate the performance of the schemes for defective input. In this respect the PDD-scheme might be more robust, as it only requires temperature as a forcing and only distinguishes between snow and ice but does not require albedo. Due to the ideal input, all schemes reproduce the year-to-year evolution of the total Greenland surface melt of the MAR-simulation reasonably well (Fig. S1 in the supplement). With intensifying surface melt rates, both, the PDD-scheme and the ETIM, yield increasing errors, which is not apparent for the dEBM (Fig. 2). On the other hand, the dEBM cannot reproduce melt rates which may still occur even though the sun does not pass over the critical elevation angle and the duration of the melt period vanishes. The root mean square error of the predicted monthly, local melt rates relative to MAR melt rates is $3.6\,\mathrm{mm\,d^{-1}}$ for the PDD scheme, $5.0\,\mathrm{mm\,d^{-1}}$ for the ETIM and $3.3\,\mathrm{mm\,d^{-1}}$ for the dEBM, if we only consider grid points and months which comply with the background melting condition of $\overline{T}_a > -6.5\,\mathrm{K}$. In comparison to the

The Cryosphere Discuss., https://doi.org/10.5194/tc-2018-130
Manuscript under review for journal The Cryosphere
Discussion started: 11 July 2018

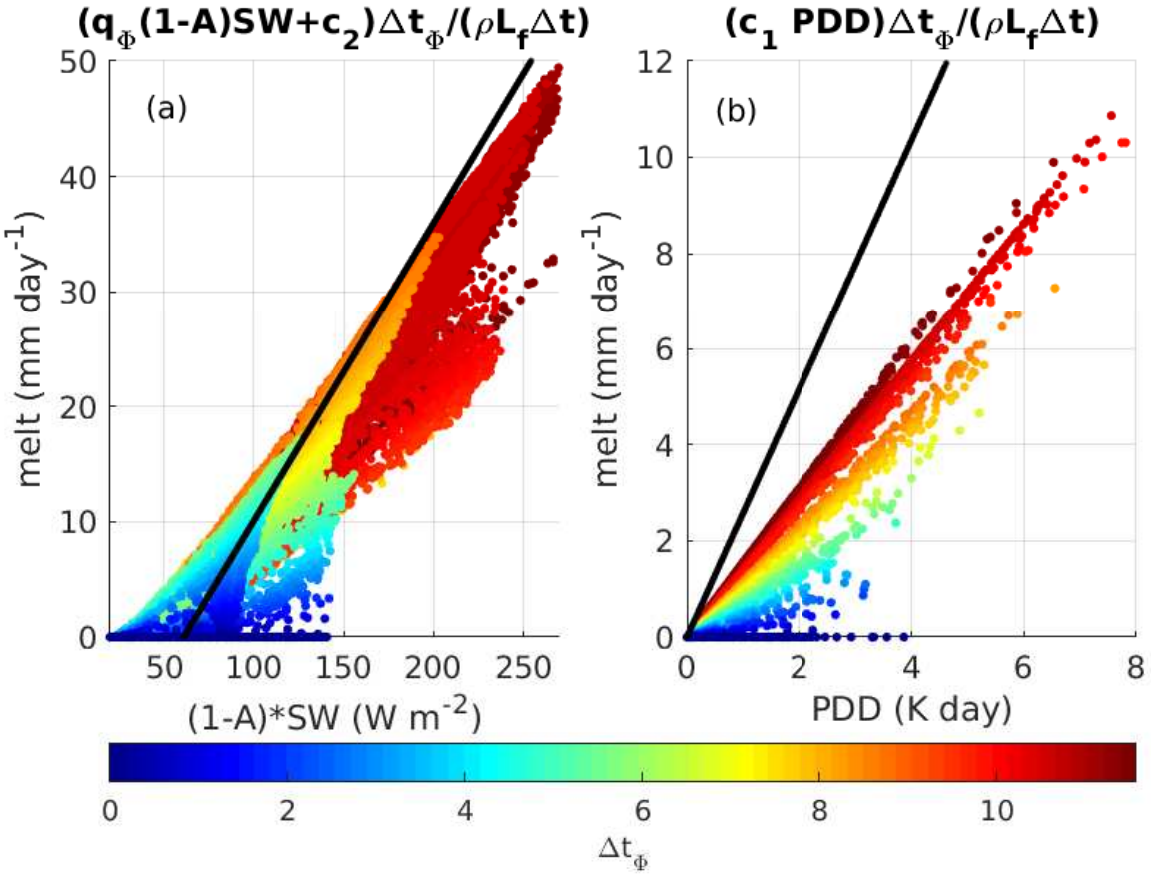

Figure 1. a) Contribution of the first and third term (radiative contribution) and b) of the second term (PDD contribution) in Eq. (6) to monthly melt rates as diagnosed with climatological temperatures and solar radiation from the MAR simulation. Colors indicate length of melt period (h). The black lines represent the respective prediction of the ETIM according to Eq. (14)

The Cryosphere Discuss., https://doi.org/10.5194/tc-2018-130
Manuscript under review for journal The Cryosphere
Discussion started: 11 July 2018

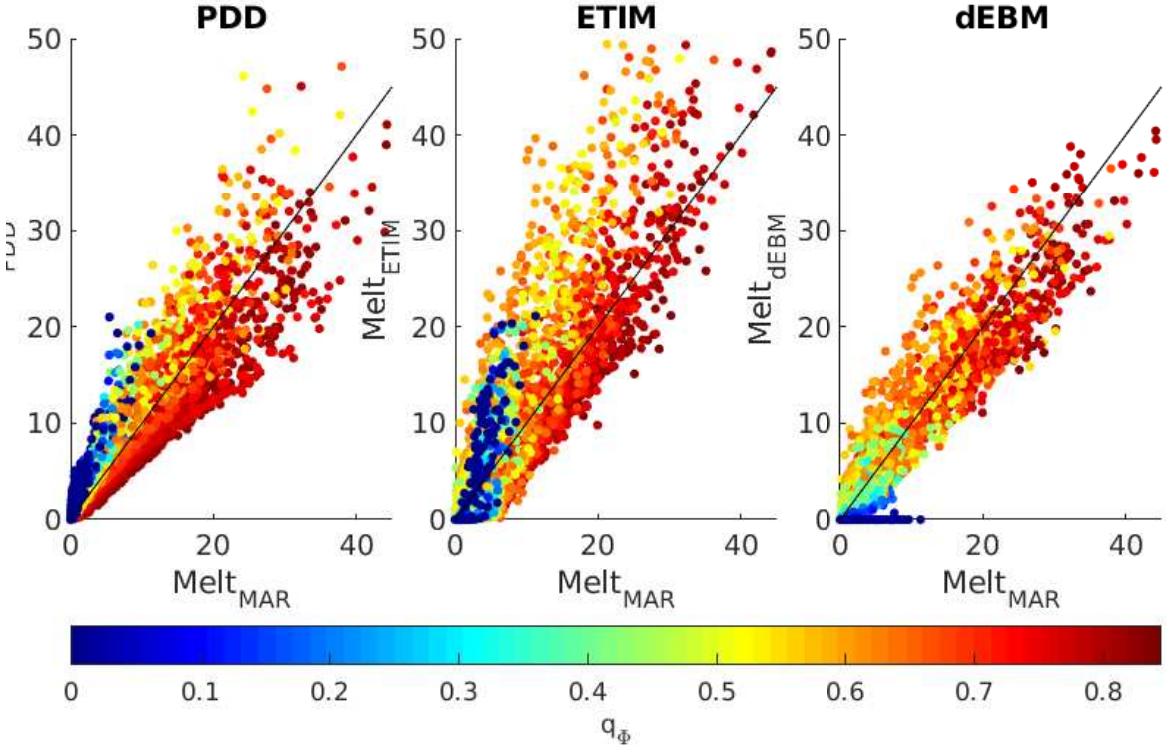

Figure 2. Multi-year monthly mean meltrates averaged of the years 1948-2016 as predicted by a) the PDD-scheme, b) the ETIM and c) the dEBM against respective MAR melt rates. Colors reflect the lenght of the daily melt period. Identity is displayed as a black line in all panels for comparison.

two empirical schemes, the dEBM produces smaller local errors with biasses being pronounced only in a narrow band along the ice sheet's margins (Fig.3).

4 Conclusions

The presented new scheme for surface melt (dEBM) requires, like enhanced temperature-index methods, monthly mean air temperatures and insolation as input, but implicitly also includes the diurnal cycle. Together with suitable schemes for albedo and refreeze (e.g. the parameterizations used together with the enhanced temperature index method in Robinson et al., 2010), it may replace empirical surface melt schemes which are commonly used in ice sheet modelling on long time scales.

The Cryosphere Discuss., https://doi.org/10.5194/tc-2018-130
Manuscript under review for journal The Cryosphere
Discussion started: 11 July 2018

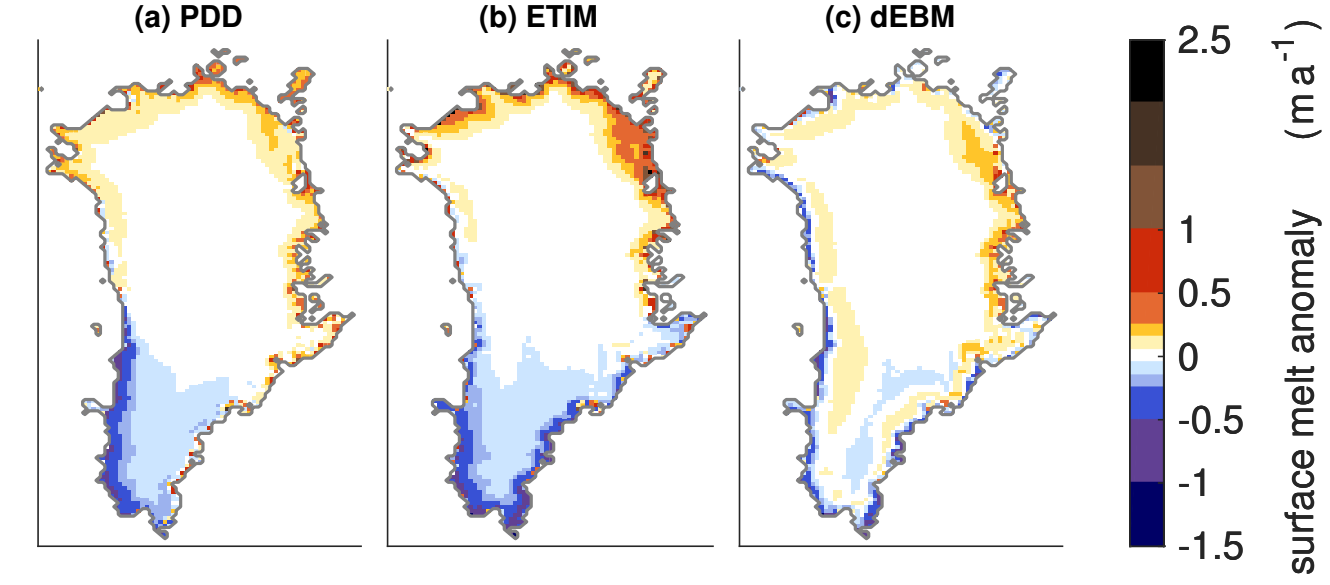

Figure 3. Bias between yearly melt rates as predicted by the individual schemes and as simulated by MAR, averaged over the whole simulation: a) PDD b) ETIM c) the proposed new scheme dEBM

An application to the Greenland Ice Sheet indicates, that the scheme may improve the spatial representation of surface melt in comparison to common empirical schemes. However, an evaluation to an independent data base is desirable. The most important advantage of the dEBM over empirical schemes may be, that it can be applied to other ice sheets and glaciers and under different climate conditions, as parameters in the scheme are physically constrained and implicitly account for the orbital configuration.

The daily melt period is defined by a minimum solar elevation angle. Together with the melt period, parameters in the dEBM depend on latitude and month of the year, but do not change from year to year if the minimum solar elevation angle is kept constant and the orbital configuration remains the same. For the Greenland Ice Sheet, a minimum solar elevation angle of $23.5°$ was roughly estimated from the mean summer insolation normal to a surface at the bottom of the atmosphere. Since the normal summer insolation depends on the orbital configurations and atmospheric transmissivity, the minimum solar elevation angle should be readjusted for applications on the southern hemisphere, accounting for the stronger austral summer insolation. On long time scales the elevation angle may also change with orbital configuration and atmospheric composition.

In the presented formulation a threshold temperature serves as a prerequisite for surface melt on monthly time scales. This threshold temperature should be considered as a tuning parameter, as the representation of the ice-atmosphere boundary layer in Earth system models may differ considerably from the MAR simulation, which here has served as a reference.

Furthermore, non-radiative heat fluxes are only crudely represented. Depending on application, it may be advisable to adapt the heat transfer coefficient to different climate regimes or to include additional atmospheric variables, such as wind speed and humidity, for a better parameterisations of turbulent heat fluxes.

The presented formulation has been designed for long Earth System Model applications, but it may be adapted to be also used in the context of climate reconstructions or to be applied on regional or local scales.

Competing interests. The authors declare that they have no competing interests

Acknowledgements. We would like to thank Xavier Fettweis for providing MAR model output.U. Krebs-Kanzow is funded by the Helmholtz Climate Initiative REKLIM (Regional Climate Change) a joint research project of the Helmholtz Association of German research centres. This work is part of the project “Global sea level change since the Mid Holocene: Background trends and climate-ice sheet feedbacks” funded from the Deutsche Forschungsgemeinschaft (DFG) as part of the Special Priority Program (SPP)-1889 "Regional Sea Level Change and Society" (SeaLevel).

References

Ahlstrom, A. P., Gravesen, P., Andersen, S. B., van As, D., Citterio, M., Fausto, R. S., Nielsen, S., Jepsen, H. F., Kristensen, S. S., Christensen, E. L., Stenseng, L., Forsberg, R., Hanson, S., Petersen, D., and Team, P. P.: A new programme for monitoring the mass loss of the Greenland ice sheet, Geological Survey of Denmark and Greenland Bulletin, pp. 61–64, 2008.

Bauer, E. and Ganopolski, A.: Comparison of surface mass balance of ice sheets simulated by positive-degree-day method and energy balance approach, Climate of the Past, 13, 819–832, https://doi.org/10.5194/cp-13-819-2017, 2017.

Box, J.: Greenland Ice Sheet Mass Balance Reconstruction. Part II: Surface Mass Balance (1840-2010), Journal of Climate, 26/18, 6974–6989, https://doi.org/10.1175/JCLI-D-12-00518.1, 2013.

Braithwaite, R.: Calculation of degree-days for glacier-climate research, Zeitschrift für Gletscherkunde und Glazialgeologie, 20/1984, 1–8, 1985.

Braithwaite, R.: Aerodynamic stability and turbulent sensible-heat flux over a melting ice surface, the Greenland Ice-Sheet, Journal of Glaciology, 41, 562–571, 1995.

Carenzo, M., Pellicciotti, F., Mabillard, J., Reid, T., and Brock, B. W.: An enhanced temperature index model for debris-covered glaciers accounting for thickness effect, Advances in Water Resources, 94, 457–469, https://doi.org/10.1016/j.advwatres.2016.05.001, 2016.

Charbit, S., Dumas, C., Kageyama, M., Roche, D. M., and Ritz, C.: Influence of ablation-related processes in the build-up of simulated Northern Hemisphere ice sheets during the last glacial cycle, Cryosphere, 7, 681–698, https://doi.org/10.5194/tc-7-681-2013, 2013.

de Boer, B., van de Wal, R. S. W., Lourens, L. J., Bintanja, R., and Reerink, T. J.: A continuous simulation of global ice volume over the past 1 million years with 3-D ice-sheet models, Climate Dynamics, 41, 1365–1384, https://doi.org/10.1007/s00382-012-1562-2, 2013.

Falk, U., Lopez, D. A., and Silva-Busso, A.: Multi-year analysis of distributed glacier mass balance modelling and equilibrium line altitude on King George Island, Antarctic Peninsula, Cryosphere, 12, 1211–1232, https://doi.org/10.5194/tc-12-1211-2018, 2018.

Fettweis, X., Box, J. E., Agosta, C., Amory, C., Kittel, C., Lang, C., van As, D., Machguth, H., and Gallee, H.: Reconstructions of the 1900-2015 Greenland ice sheet surface mass balance using the regional climate MAR model, Cryosphere, 11, 1015–1033, https://doi.org/10.5194/tc-11-1015-2017, 2017.

Gierz, P., Lohmann, G., and Wei, W.: Response of Atlantic overturning to future warming in a coupled atmosphere-ocean-ice sheet model, Geophysical Research Letters, 42, 6811–6818, https://doi.org/10.1002/2015GL065276, 2015.

Heinemann, M., Timmermann, A., Timm, O. E., Saito, F., and Abe-Ouchi, A.: Deglacial ice sheet meltdown: orbital pacemaking and CO2 effects, Climate of the Past, 10, 1567–1579, https://doi.org/10.5194/cp-10-1567-2014, 2014.

Kalnay, E., Kanamitsu, M., Kistler, R., Collins, W., Deaven, D., Gandin, L., Iredell, M., Saha, S., White, G., Woollen, J., Zhu, Y., Chelliah, M., Ebisuzaki, W., Higgins, W., Janowiak, J., Mo, K., Ropelewski, C., Wang, J., Leetmaa, A., Reynolds, R., Jenne, R., and Joseph, D.: The NCEP/NCAR 40-year reanalysis project, Bulletin of the American Meteorological Society, 77, 437–471, https://doi.org/10.1175/1520-0477(1996)077<0437:TNYRP>2.0.CO;2, 1996.

Krapp, M., Robinson, A., and Ganopolski, A.: SEMIC: an efficient surface energy and mass balance model applied to the Greenland ice sheet, Cryosphere, 11, 1519–1535, https://doi.org/10.5194/tc-11-1519-2017, 2017.

Krebs-Kanzow, U., Gierz, P., and Lohmann, G.: Estimating Greenland surface melt is hampered by melt induced dampening of temperature variability, Journal of Glaciology, 64, 227–235, https://doi.org/10.1017/jog.2018.10, 2018.

Liou, K. N.: An introduction to atmospheric radiation, Academic Press, second edition edn., 2002.

Pellicciotti, F., Brock, B., Strasser, U., Burlando, P., Funk, M., and Corripio, J.: An enhanced temperature-index glacier melt model including the shortwave radiation balance: development and testing for Haut Glacier d'Arolla, Switzerland, JOURNAL OF GLACIOLOGY, 51, 573–587, https://doi.org/10.3189/172756505781829124, 2005.

Pollard, D.: A simple parameterization for ice sheet ablation rate, Tellus, 32, 384–388, https://doi.org/10.1111/j.2153-3490.1980.tb00965.x, 1980.

Reeh, N.: Parameterization of melt rate and surface temperature on the Greenland ice sheet, Polarforschung, 59, 113–128, 1989.

Robinson, A., Calov, R., and Ganopolski, A.: An efficient regional energy-moisture balance model for simulation of the Greenland Ice Sheet response to climate change, The Cryosphere, 4, 129–144, https://doi.org/https://doi.org/10.5194/tc-4-129-2010, 2010.

Roche, D. M., Dumas, C., Bugelmayer, M., Charbit, S., and Ritz, C.: Adding a dynamical cryosphere to iLOVECLIM (version 1.0): coupling with the GRISLI ice-sheet model, Geoscientific Model Development, 7, 1377–1394, https://doi.org/10.5194/gmd-7-1377-2014, 2014.

Sasgen, I., van den Broeke, M., Bamber, J. L., Rignot, E., Sorensen, L. S., Wouters, B., Martinec, Z., Velicogna, I., and Simonsen, S. B.: Timing and origin of recent regional ice-mass loss in Greenland, Earth and Planetary Science Letters, 333, 293–303, https://doi.org/10.1016/j.epsl.2012.03.033, 2012.

Tapley, B., Bettadpur, S., Ries, J., Thompson, P., and Watkins, M.: GRACE measurements of mass variability in the Earth system, Science, 305, 503–505, https://doi.org/10.1126/science.1099192, 2004.

Tedesco, M. and Fettweis, X.: 21st century projections of surface mass balance changes for major drainage systems of the Greenland ice sheet, Environmental Research Letters, 7, https://doi.org/10.1088/1748-9326/7/4/045405, 2012.

van den Berg, J., van de Wal, R., and Oerlemans, H.: A mass balance model for the Eurasian ice sheet for the last 120,000 years, Global and Planetary Change, 61, 194–208, https://doi.org/10.1016/j.gloplacha.2007.08.015, 2008.

Wilton, D. J., Jowett, A., Hanna, E., Bigg, G. R., van den Broeke, M. R., Fettweis, X., and Huybrechts, P.: High resolution (1 km) positive degree-day modelling of Greenland ice sheet surface mass balance, 1870-2012 using reanalysis data, Journal of Glaciology, 63, 176–193, https://doi.org/10.1017/jog.2016.133, 2017.

Wouters, B., Bonin, J. A., Chambers, D. P., Riva, R. E. M., Sasgen, I., and Wahr, J.: GRACE, time-varying gravity, Earth system dynamics and climate change, Reports on Progress in Physics, 77, https://doi.org/10.1088/0034-4885/77/11/116801, 2014.

Zemp, M., Frey, H., Gärtner-Roer, I., Nussbaumer, S. U., Hoelzle, M., Paul, F., Haeberli, W., Denzinger, F., Ahlstrøm, A. P., Anderson, B., and et al.: Historically unprecedented global glacier decline in the early 21st century, Journal of Glaciology, 61, 745–762, https://doi.org/10.3189/2015JoG15J017, 2015.

Ziemen, F. A., Rodehacke, C. B., and Mikolajewicz, U.: Coupled ice sheet-climate modeling under glacial and pre-industrial boundary conditions, Climate of the Past, 10, 1817–1836, https://doi.org/10.5194/cp-10-1817-2014, 2014.

https://doi.org/10.5194/tc-0-1-2018-supplement